Generalized Correlation Profiles in Single-File Systems

Alexis Poncet,[1,3] Aurélien Grabsch,[1] Pierre Illien,[2] and Olivier Bénichou[1,*]
[1]Sorbonne Université, CNRS, Laboratoire de Physique Théorique de la Matière Condensée (LPTMC), 4 Place Jussieu, 75005 Paris, France
[2]Sorbonne Université, CNRS, Laboratoire de Physico-Chimie des Électrolytes et Nanosystèmes Interfaciaux (PHENIX), 4 Place Jussieu, 75005 Paris, France
[3]Univ. Lyon, ENS de Lyon, Univ. Claude Bernard, CNRS, Laboratoire de Physique, F-69342 Lyon, France

(Received 4 June 2021; revised 15 October 2021; accepted 15 October 2021; published 24 November 2021)

Single-file diffusion refers to the motion in narrow channels of particles which cannot bypass each other, and leads to tracer subdiffusion. Most approaches to this celebrated many-body problem were restricted to the description of the tracer only. Here, we go beyond this standard description by introducing and providing analytical results for generalized correlation profiles (GCPs) in the frame of the tracer. In addition to controlling the statistical properties of the tracer, these quantities fully characterize the correlations between the tracer position and the bath particles density. Considering the hydrodynamic limit of the problem, we determine the scaling form of the GCPs with space and time, and unveil a nonmonotonic dependence with the distance to the tracer despite the absence of any asymmetry. Our analytical approach provides several exact results for the GCPs for paradigmatic models of single-file diffusion, such as Brownian particles with hardcore repulsion, the symmetric exclusion process and the random average process. The range of applicability of our approach is further illustrated by considering (i) extensions to general interactions between particles, (ii) the out-of-equilibrium situation of an initial step of density, and (iii) beyond the hydrodynamic limit, the GCPs at arbitrary time in the dense limit.

DOI: 10.1103/PhysRevLett.127.220601

The key feature of single-file diffusion [1–3], which refers to the motion of particles which cannot bypass each other, is that a typical displacement of a tracer particle scales as $t^{1/4}$ instead of $t^{1/2}$ as in regular diffusion [4–11]. This subdiffusive scaling has been demonstrated in a growing number of experimental realizations, in contexts as varied as transport in porous media [12,13], zeolites [14], or confined colloidal suspensions [15,16]. Theoretically, it has lead to a huge number of works in the physical and mathematical literature. Recent advances include the determination of the large deviation functions of the position of a tracer in a system of Brownian particles with hardcore repulsion [17–19] and in the symmetric exclusion process [20,21] (see below for definitions), which are two paradigmatic models of single-file diffusion with hard-core interactions.

Theoretical interest in single-file diffusion originates from the challenging many-body nature of the problem: any large displacement of the tracer particle in one direction requires large displacements of more and more bath particles in the same direction. However, the quantification of the coupling between the tracer position and the bath particles density remains a broadly open question. Here, we develop a theoretical framework with which to determine these correlations for single-file systems.

We introduce our formalism by considering first the symmetric exclusion process (SEP). Particles, present at a density ρ, perform symmetric continuous-time random walks on a one-dimensional lattice with unit jump rate, and hard-core exclusion is enforced by allowing at most one particle per site [Fig. 1(a)]. The tracer, of position X_t at

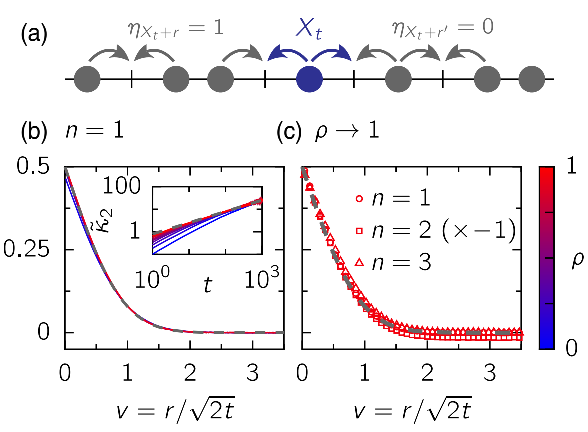

FIG. 1. SEP. (a) The symmetric exclusion process (SEP). The position of the tracer is called X_t and the occupation numbers of the sites with respect to the tracer are denoted η_{X_t+r}. (b) Profiles of order 1 at densities 0.1,0.25,0.5,0.75,0.9 at time $t = 3000$ (blue to red). Dashed gray line: prediction from Eq. (9). Inset: rescaled variance $\tilde{\kappa}_2 = \kappa_2 \rho/(1-\rho)$ compared to known expression (gray) [7] and retrieved by our approach. (c) Profiles of order 1, 2, and 3 at high density ($\rho = 0.95$, $t = 1000$). Dashed gray line: prediction from Eq. (10).

 © 2021 American Physical Society

time t, is initially at the origin. The bath particles are described by the set of occupation numbers $\eta_r(t)$ of each site $r \in \mathbb{Z}$ of the line at time t, with $\eta_r(t) = 1$ if the site is occupied and $\eta_r(t) = 0$ otherwise.

To quantify the coupling between the position of the tracer and the density of bath particles, we study the joint process (X_t, η_{X_t+r}), which is entirely characterized by its joint cumulant generating function $\ln\langle e^{\lambda X_t + \chi \eta_{X_t+r}}\rangle$. Since η_{X_t+r} only takes values 0 and 1, this function takes the form [22]

$$\ln\langle e^{\lambda X_t + \chi \eta_{X_t+r}}\rangle = \psi(\lambda, t) + \ln(1 + (e^{\chi} - 1) w_r(\lambda, t)), \qquad (1)$$

where $\psi(\lambda, t)$ is the usual cumulant-generating function, whose expansion defines the cumulants κ_n of the position:

$$\psi(\lambda, t) \equiv \ln\langle e^{\lambda X_t}\rangle \equiv \sum_{n=1}^{\infty} \frac{\lambda^n}{n!} \kappa_n(t). \qquad (2)$$

In turn, $w_r(\lambda, t)$ is the generalized correlation profile (GCP)-generating function [27,28]

$$w_r(\lambda, t) = \langle \eta_{X_t+r} e^{\lambda X_t}\rangle / \langle e^{\lambda X_t}\rangle, \qquad (3)$$

whose expansion gives the joint cumulants $\langle \eta_{X_t+r} X_t^n\rangle_c$ of the tracer position X_t and the occupation number η_{X_t+r} measured in its frame of reference. For instance, the first cumulant $\langle \eta_{X_t+r} X_t\rangle_c = \mathrm{Cov}(\eta_{X_t+r}, X_t)$ provides a measure of the correlations between the displacement of the tracer and the occupation of the site at a distance r of the tracer, while the second one $\langle \eta_{X_t+r} X_t^2\rangle_c = \mathrm{Cov}(\eta_{X_t+r}, X_t^2)$ (since $\langle X_t\rangle = 0$) gives a measure of the correlation between the amplitude of the fluctuations of X_t and the occupation at a distance r of X_t. Finally, the joint cumulant generating function (1) is given by the knowledge of ψ and w_r, which are thus key quantities, whose joint determination is the object of this Letter.

While it is known that the cumulant-generating function ψ scales as $\sqrt{t}$ at large time for single-file systems, we put forward that, more generally, at large scale (large time, large distances), the GCP-generating function admits the scaling form:

$$w_r(\lambda, t) - \rho \underset{t\to\infty}{\sim} \Phi\left(\lambda, v = \frac{r}{\sqrt{2t}}\right) \equiv \sum_{n=1}^{\infty} \frac{\lambda^n}{n!} \Phi_n(v). \qquad (4)$$

We note that the symmetry of the system imposes $\Phi(\lambda, v) = \Phi(-\lambda, -v)$: in the following the results will be stated only for $v > 0$. When the tracer moves, it perturbs the bath particles and gives birth to correlation profiles which, as displayed by this scaling form, are not stationary but involve typical length scales growing as $\sqrt{t}$. In turn, the way the bath particles readjust at the front and behind the tracer (encoded in $w_{\pm 1}$) controls its displacement. This can be quantified by computing the time evolution of the cumulant generating function ψ, using a mixed Eulerian (for the bath particles) and Lagrangian (for the tracer) master equation, leading to (see Sec. I in the Supplemental Material, SM [22])

$$\frac{d\psi}{dt} = \frac{1}{2}[(e^{\lambda} - 1)(1 - w_1) + (e^{-\lambda} - 1)(1 - w_{-1})]. \qquad (5)$$

Finally, this equation shows that, besides fully quantifying the correlations between the tracer position and the density of bath particles, the GCPs control the time evolution of the cumulant-generating function. In particular, the scaling $\psi(\lambda, t) \underset{t\to\infty}{\sim} \sqrt{t}$ of the cumulants [20,21] actually originates from the scaling form (4) of the GCP generating function. Relying again on the mixed Eulerian and Lagrangian master equation and on the scaling of Φ [Eq. (4)], we show in the SM that this key quantity satisfies the hydrodynamic equation

$$\Phi''(v) + 2(v + b_\mu)\Phi'(v) + C(v) = 0 \qquad (6)$$

completed by the boundary conditions

$$\Phi'(0^{\pm}) + 2b_{\pm}[\rho + \Phi(0^{\pm})] = 0 \qquad (7)$$

$$1 - \rho - \Phi(0^-) = e^{\lambda}[1 - \rho - \Phi(0^+)] \qquad (8)$$

in front and past the tracer, with μ the sign of v, $b_\mu(\lambda) \equiv \lim_{t\to\infty}\psi(\lambda, t)/[\sqrt{2t}(e^{\mu\lambda} - 1)]$ and the dependence on λ omitted for simplicity. While Eq. (7) results from the time evolution of $w_{\pm 1}$ obtained from the master equation, Eq. (8) comes from the cancellation of $(d\psi/dt)$ at large times [see Eq. (5)] due to the scaling $\psi(\lambda, t) \sim \sqrt{t}$. The function $C(v)$ involves higher order correlations, and is *a priori* unknown. However, as we report below (see SM for details), explicit exact expressions of the GCPs can be obtained in several important situations.

First, we show that the function $C(v)$ is strictly equal to zero at first order in λ, making Eq. (6) closed at this order, and leading to

$$\Phi_1(v > 0) = \frac{1 - \rho}{2} \mathrm{erfc}(v). \qquad (9)$$

This expression provides the exact large-time behavior of the correlation function $\langle \eta_{X_t+r} X_t\rangle_c = \mathrm{Cov}(\eta_{X_t+r}, X_t)$ of the SEP at any density. The fact that it is positive for $v > 0$ indicates that, if $X_t > 0$, the sites to the right of the tracer have higher occupation numbers, which shows that there is an accumulation of particles in front of the tracer. Note that it decays monotonically to zero with the distance to the tracer [Fig. 1(b)]. We finally stress that (9) together with (8) allows one to recover in a straightforward way the well-known expression of the second cumulant $\kappa_2(t) = (1-\rho)/\rho\sqrt{2t/\pi}$ [4].

Second, in the dense limit $\rho \to 1$, it is shown that the function $C(v)$, which involves a product of occupation numbers of bath particles, vanishes, which leads to the full GCP-generating function

$$\lim_{\rho\to 1} \frac{\Phi(\lambda, v > 0)}{1-\rho} = \frac{1-e^{-\lambda}}{2} \mathrm{erfc}(v), \tag{10}$$

where the dependencies on λ and v factorize. This expression gives the GCPs of arbitrary order, which, up to a sign, assume all the same value, and again decay monotonically to zero [Fig. 1(c)].

Third we investigate the dilute limit $\rho \to 0$ of the SEP. We stress that the results in this case cannot be deduced from the dense limit discussed above, since the particle-hole symmetry of the SEP is explicitly broken by choosing to follow the motion of one particle. Actually, this limit exhibits a richer phenomenology. In fact, it corresponds to the model of interacting pointlike particles on a line [17–19], and needs to be taken at constant $x = \rho r$ and $\tau = \rho^2 t$. The density field $\eta_{X_t+r}(t) \mapsto \eta(x,\tau)$ becomes continuous in space and the diffusive scaling for the GCPs reads $v = r/\sqrt{2t} = x/\sqrt{2\tau}$, leading to the definition $\hat{\Phi}(\hat{\lambda}, v) = \lim_{\rho\to 0}[\Phi(\lambda = \rho\hat{\lambda}, v)/\rho]$. In this case, the function $C(v)$ is not negligible, but we put forward self-consistently, in order to retrieve the known cumulants κ_n (see point (i) below), the closure relation

$$\lim_{\rho\to 0}[C(\lambda = \rho\hat{\lambda}, v)/\rho] = 2\hat{\lambda}\frac{d\beta}{d\hat{\lambda}}\hat{\Phi}'(v), \tag{11}$$

where we defined $\beta = \lim_{t\to\infty}(1/\sqrt{2t})(\hat{\psi}/\hat{\lambda})$, with $\hat{\psi}(\hat{\lambda}) = \lim_{\rho\to 0}[\psi(\lambda = \rho\hat{\lambda})/\rho]$. This leads to the key and strikingly simple closed equation for the full GCP-generating function

$$\hat{\Phi}''(v) + 2(v+\xi)\hat{\Phi}'(v) = 0, \tag{12}$$

which is the main result of this Letter. Together with (7), it yields

$$\hat{\Phi}(\hat{\lambda}, v > 0) = \frac{\beta \mathrm{erfc}(v+\xi)}{\pi^{-1/2}e^{-\xi^2} - \beta\mathrm{erfc}(\xi)}, \tag{13}$$

where $\xi = \lim_{t\to\infty}(1/\sqrt{2t})(d\hat{\psi}/d\hat{\lambda})$. The quantities β and $\xi = (d/d\hat{\lambda})(\hat{\lambda}\beta)$ are then determined from Eq. (8), which becomes

$$\beta \sum_{\mu=\pm 1} \frac{\mathrm{erfc}(\mu\xi)}{\pi^{-1/2}e^{-\xi^2} - \mu\beta\mathrm{erfc}(\mu\xi)} = \hat{\lambda}. \tag{14}$$

Several comments are in order. (i) Equation (14) is an implicit equation that allows one to retrieve the exact cumulants κ_n obtained in previous studies [17–19] (see Sec. II.C in the SM [22] for detailed correspondence). This validates self-consistently the closure relation (11). (ii) Then, Eq. (13) provides the GCPs of interacting pointlike particles at arbitrary order; for instance (Fig. 2),

$$\Phi_2(v) = \frac{1}{\rho}\left[\frac{1}{2}\mathrm{erfc}v - 2\frac{e^{-v^2}}{\pi}\right], \tag{15}$$

$$\Phi_3(v) = \frac{3}{\pi^{3/2}\rho^2}[(2v - \sqrt{\pi})e^{-v^2} + \sqrt{\pi}\mathrm{erfc}v]. \tag{16}$$

(iii) The sign of these GCPs is nontrivial. For instance, $\Phi_2(v) = \mathrm{Cov}(\eta_{X_t+r}, X_t^2)$ is negative (see Fig. 2 for $n = 2$), which implies that X_t^2 and η_{X_t+r} fluctuate in opposite directions: a larger fluctuation of X_t^2 is associated with a smaller value of the occupation. Furthermore, even if there is no asymmetry in the dynamics, these GCPs display a surprising nonmonotonic behavior with the distance to the tracer (see Fig. 2 for $n \geq 2$), which indicates that this effect is more pronounced at a certain distance of the tracer (which is non stationary, and grows as $\sqrt{t}$). (iv) It is demonstrated in Sec. III.C in the SM [22] that the GCPs actually coincide with the saddle-point solution in the formalism of macroscopic fluctuation theory (MFT) [35], evaluated at a specific point. In turn, it sheds new light on this saddle-point solution. This, after (i), is a further validation of the exactness of the closure relation (11). A key result of our approach is that the GCPs satisfy the very simple closed equation (12). (v) We stress that our approach can be generalized to the important out-of-equilibrium situation of an initial step of density [21,36]. The main equation (12) remains valid in this case, and only the boundary conditions [(7), (8)] must be straightforwardly adapted. The modified equations, and explicit expressions of the cumulants and the GCPs are given in the SM [22] [Eqs. (S58–S65)].

These analytical results can also be extended to a general single-file system of interacting particles with average density ρ. Such a system can be described at large scale by two quantities: the collective diffusion coefficient $D(\rho)$ and the static structure factor at vanishing wave number $S(\rho)$ [16,34,37,38]. The case of the SEP considered above corresponds to $D(\rho) = 1/2$ and $S(\rho) = 1-\rho$. We conjecture that the first-order GCP of a general single-file system can be obtained by adapting the main equation (12) into $D(\rho)\Phi_1''(v) + v\Phi_1'(v) = 0$, with the boundary conditions $2D(\rho)\Phi_1'(0^\pm) + \rho\tilde{\kappa}_2 = 0$ and $\Phi_1(0^+) - \Phi_1(0^-) = S(\rho)$. This leads to the general expression

$$\Phi_1(v \geq 0) = \frac{S(\rho)}{2}\mathrm{erfc}\left(\frac{v}{\sqrt{2D(\rho)}}\right). \tag{17}$$

Note that the known expression of the variance of the tracer $\kappa_2(t) = [S(\rho)/\rho]\sqrt{4D(\rho)t/\pi}$ [34,38] is recovered from the particular value $\Phi_1(0)$. The analytical result (17) can be

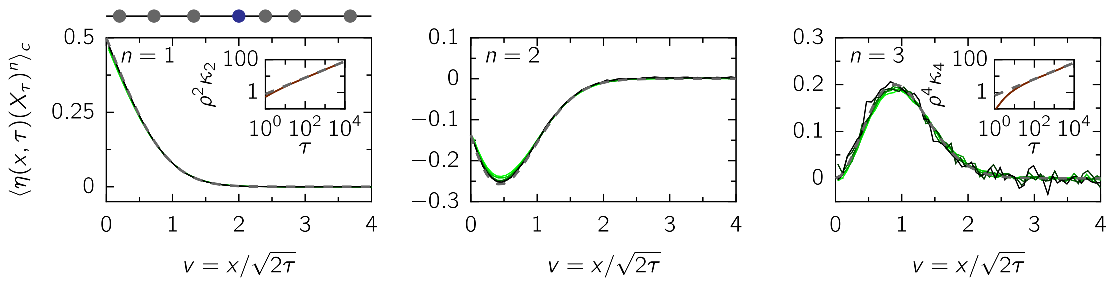

FIG. 2. Pointlike interacting particles. Rescaled orders 1, 2, and 3 (left to right) of the GCPs at times $\tau = 100, 200, 500, 1000, 2000, 5000$ (green to black). The dashed gray lines are the predictions from Eqs. (9), (15), and (16). The insets show the second and fourth cumulants with the solid lines corresponding to the simulations and the dashed gray line to the solution from Eq. (14).

retrieved by a MFT computation provided in Sec. III.C in the SM [22]. Furthermore, it is supported by numerical simulations (Fig. 3) of several paradigmatic examples of single-file systems (see caption of Fig. 3 and Sec. IV in the SM [22] for definitions) with hard-core interactions (the Brownian hard-rods model, Fig. 3(a), as involved in the experimental realization of the quasi-1D colloidal suspension from [16], and the random average process, Fig. 3(b) [32,33,39,40]) and more general pairwise interactions (Brownian pointlike particles with Weeks-Chandler-Anderson (WCA) potential Fig. 3(c), and dipole-dipole interactions, Fig. 3(d), as involved in the experimental realisation of paramagnetic colloids confined in a 1D channel from [15]).

Higher order GCPs can also be obtained in the dilute limit. Indeed, in the limit $\rho \to 0$ of a generic single-file system, the collective diffusion coefficient and the structure factor should respectively satisfy $D(\rho) \to D_0$ and $S(\rho) \to 1$ where D_0 is the diffusion constant of an individual particle and 1 is the structure factor of the ideal gas. Equations (13)–(16) are therefore valid for such a system at low enough density, as confirmed by numerical simulations [Figs. 3(e) and 3(f)].

Although we mostly focused on the hydrodynamic limit, we stress that our approach also provides a framework to analyze the GCP-generating function (3) at all times. Starting from the microscopic equation satisfied by w_r deduced from the master equation [see Eq. (S69) and (S70)

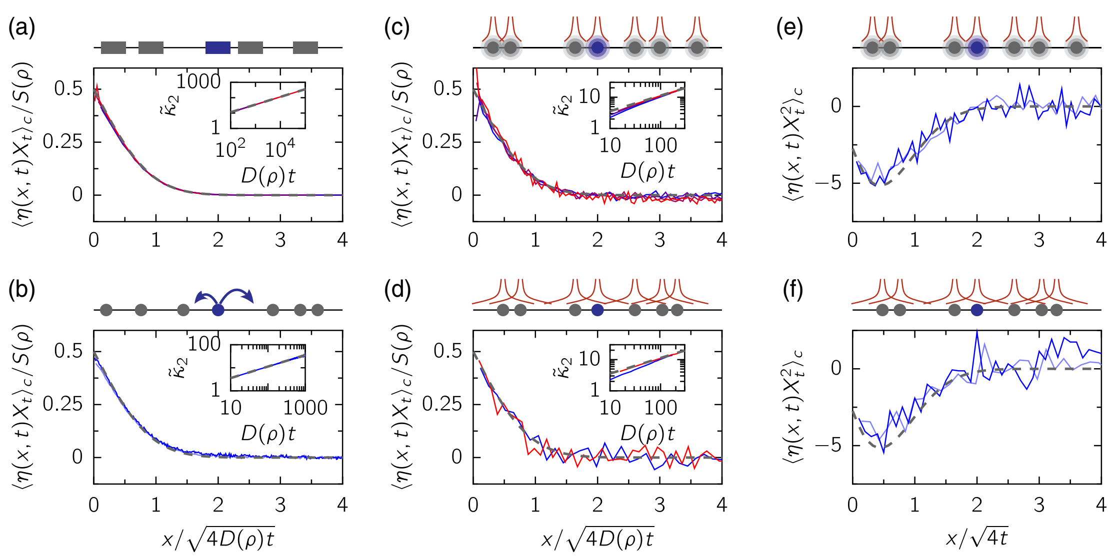

FIG. 3. GCPs of single-file systems. (a)–(d) Profiles at order 1 for various models. The dashed gray lines correspond to the prediction of Eq. (17). The insets show the rescaled variance $\tilde{\kappa}_2 = \kappa_2\rho/S(\rho)$ with the prediction in gray. (a) Hard-rod gas at density $\rho = 1$ and time $t = 1000$. The length of a rod is $a = 0.1, 0.25, 0.5, 0.75, 0.9$ (blue to red). The parameters are $S(\rho) = (1 - a\rho)^2$, $D(\rho) = (1 - a\rho)^{-2}$ [16]. (b) Random-average process [32,33] at density $\rho = 1$ at times $t = 1000$ and 5000 (light blue and blue): at exponential times, each particle performs a symmetric jump whose length is a random fraction of the distance to the nearest particle. $S(\rho)$ and $D(\rho)$ are given in Ref. [33]. (c) Pointlike Brownian particles interacting by a Weeks-Chandler-Andersen potential [$V(r) \propto [(1/r^{12}) - (1/r^6)]$ for $r < 2^{1/6}$ and 0 otherwise]. Density $\rho = 0.2, 0.3, 0.4, 0.5$ (blue to red) at time $t = 100$. $S(\rho)$ is the structure factor at vanishing wave-number, and $D(\rho) = D_0/S(\rho)$ [16,34]. (d) Pointlike Brownian particles interacting with long-range dipole-dipole interactions $V(r) \propto (1/r^3)$ at density $\rho = 0.2$ and 0.4 (blue and red) at time $t = 100$. (e),(f) Profiles of order 2 for the same models as (c),(d) at density $\rho = 0.05$ and times 5×10^3 and 1×10^4 (light blue and blue). The dashed gray line is the low-density prediction from Eq. (15).

in the SM], the dense limit of the GCP-generating function $\check{w}_r = \lim_{\rho\to 1}(w_r - \rho)/(1-\rho)$ in the Laplace domain reads

$$\tilde{w}_r(u) = \int_0^\infty e^{-ut}\check{w}_r(t)dt = \frac{1}{u}\frac{1-e^{-\nu\lambda}}{1+\alpha}\alpha^{|r|}, \quad (18)$$

where $\nu = \mathrm{sign}(r)$ and $\alpha = 1+u-\sqrt{(1+u)^2-1}$, and the dense limit of the cumulant generating function at all times $\check{\psi}(\lambda,t) = \lim_{\rho\to 1}\psi/(1-\rho) = te^{-t}(I_0(t)+I_1(t))[\cosh\lambda - 1]$, where I_n is a modified Bessel function of order n.

All together, the theoretical framework developed in this Letter allows one to quantify the correlations between the tracer and the bath of particles in single-file diffusion with the help of generalized correlation profiles. We emphasize the main merits of this method. First, it is based on a master equation, which is a natural tool for physicists. Second, in the limits considered here, it reduces to a simple first order linear differential equation. In views of the complexity of available methods to study tracer diffusion in single-file systems, such as the coupled nonlinear partial differential equation for the macroscopic fluctuation theory [17,35] or integrable probabilities and the Bethe ansatz [21], this is an important simplification. Furthermore, we discover a closure relation which allows us to break the infinite hierarchy in a many-body model of pointlike particles with hardcore repulsion. Beyond these technical aspects, the impact of the present results is further demonstrated by considering extensions to general interactions between particles, the out-of-equilibrium situation of an initial step of density and, beyond the hydrodynamic limit, the GCPs at arbitrary time in the dense limit. Finally, our method opens the way to the resolution at arbitrary density, which is a long-standing and challenging question.

*Corresponding author.
benichou@lptmc.jussieu.fr

[1] T. Chou, K. Mallick, and R. K. P. Zia, Rep. Prog. Phys. **74**, 116601 (2011).
[2] K. Mallick, Physica (Amsterdam) **418A**, 17 (2015).
[3] P. Krapivski, S. Redner, and E. Ben-Naim, *A Kinetic View of Statistical Physics* (Cambridge University Press, Cambridge, England, 2009).
[4] T. E. Harris, J. Appl. Probab. **2**, 323 (1965).
[5] D. G. Levitt, Phys. Rev. A **8**, 3050 (1973).
[6] S. Alexander and P. Pincus, Phys. Rev. B **18**, 2011 (1978).
[7] R. Arratia, Ann. Probab. **11**, 362 (1983).
[8] C. Rödenbeck, J. Kärger, and K. Hahn, Phys. Rev. E **57**, 4382 (1998).
[9] A. Taloni and M. A. Lomholt, Phys. Rev. E **78**, 051116 (2008).
[10] A. Taloni, A. Chechkin, and J. Klafter, Phys. Rev. E **84**, 021101 (2011).
[11] A. Taloni and F. Marchesoni, Biophys. Rev. Lett. **09**, 381 (2014).
[12] V. Gupta, S. S. Nivarthi, A. V. McCormick, and H. Ted Davis, Chem. Phys. Lett. **247**, 596 (1995).
[13] T. Meersmann, J. W. Logan, R. Simonutti, S. Caldarelli, A. Comotti, P. Sozzani, L. G. Kaiser, and A. Pines, J. Phys. Chem. A **104**, 11665 (2000).
[14] K. Hahn, J. Kärger, and V. Kukla, Phys. Rev. Lett. **76**, 2762 (1996).
[15] Wei, Bechinger, and Leiderer, Science **287**, 625 (2000).
[16] B. Lin, M. Meron, B. Cui, S. A. Rice, and H. Diamant, Phys. Rev. Lett. **94**, 216001 (2005).
[17] P. L. Krapivsky, K. Mallick, and T. Sadhu, Phys. Rev. Lett. **113**, 078101 (2014).
[18] C. Hegde, S. Sabhapandit, and A. Dhar, Phys. Rev. Lett. **113**, 120601 (2014).
[19] T. Sadhu and B. Derrida, J. Stat. Mech. 09 (2015) P09008.
[20] P. Illien, O. Bénichou, C. Mejía-Monasterio, G. Oshanin, and R. Voituriez, Phys. Rev. Lett. **111**, 038102 (2013).
[21] T. Imamura, K. Mallick, and T. Sasamoto, Phys. Rev. Lett. **118**, 160601 (2017).
[22] See Supplemental Material at http://link.aps.org/supplemental/10.1103/PhysRevLett.127.220601 for details about analytical computations and numerical simulations, which includes Refs. [23–26].
[23] B. Derrida and A. Gerschenfeld, J. Stat. Phys. **137**, 978 (2009).
[24] J.-P. Hansen and I. R. McDonald, *Theory of Simple Liquids: With Applications to Soft Matter* (Academic Press, New York, 2013).
[25] H. Spohn, J. Phys. A **16**, 4275 (1983).
[26] C. Landim, S. Olla, and S. B. Volchan, Commun. Math. Phys. **192**, 287 (1998).
[27] P. Illien, O. Bénichou, G. Oshanin, and R. Voituriez, J. Stat. Mech. 11 (2015) P11016.
[28] Note that the GCP-generating function (3) can be thought as the average occupation in a biaised ensemble. This type of objects has received a lot of attention over the last years [29–31].
[29] H. Touchette, J. Stat. Phys. **159**, 987 (2015).
[30] R. Chetrite and H. Touchette, Ann. Inst. Henri Poincaré **16**, 2005 (2015).
[31] B. Derrida and T. Sadhu, J. Stat. Phys. **176**, 773 (2019).
[32] R. Rajesh and S. N. Majumdar, Phys. Rev. E **64**, 036103 (2001).
[33] A. Kundu and J. Cividini, Europhys. Lett. **115**, 54003 (2016).
[34] M. Kollmann, Phys. Rev. Lett. **90**, 180602 (2003).
[35] P. L. Krapivsky, K. Mallick, and T. Sadhu, J. Stat. Phys. **160**, 885 (2015).
[36] B. Derrida and A. Gerschenfeld, J. Stat. Phys. **136**, 1 (2009).
[37] B. Derrida, J. Stat. Mech. 07 (2007) P07023.
[38] P. L. Krapivsky, K. Mallick, and T. Sadhu, J. Stat. Mech. 09 (2015) P09007.
[39] P. Ferrari and L. Fontes, Electron. J. Pro **3**, 1 (1998).
[40] G. M. Schütz, J. Stat. Phys. **99**, 1045 (2000).